PEER REVIEWED

Development of ScSZ Electrolyte by Very Low Pressure Plasma Spraying for High-Performance Metal-Supported SOFCs

Yue-peng Wang[1] · Jiu-tao Gao[1] · Wei Chen[1] · Cheng-xin Li[1] · Shan-lin Zhang[1] ·
Guan-jun Yang[1] · Chang-jiu Li[1]

Abstract Very low pressure plasma spraying (VLPPS) is an attractive method for metal-supported solid oxide fuel cells, wherein it can significantly avoid the oxidation of metal substrate. In this study, scandia-stabilized zirconia electrolyte was fabricated by VLPPS. To investigate the microstructure of coatings, the spraying distances were set to 150, 250 and 350 mm. The fractured morphology suggests that, at a relatively low deposition temperature ($< 350\ °C$), typical lamellar structure was replaced by trans-granular structure. The apparent porosity of coatings ranges from 4.75 to 6.83%, as per the image analysis method. The ionic conductivity of coating at 250 mm was $0.068\ \text{S cm}^{-1}$, which was $\sim 68\%$ of bulk. The ratio of surface area to projected area of coatings surface could reach 6.53-8.30 measured by a 3D confocal laser microscope. Finally, testing cells showed a maximum output power density of $1112\ \text{mW cm}^{-2}$ and an OCV of $1.07\ \text{V}$ at 750 °C. The ohmic resistance of whole cell was $0.1\ \Omega\ \text{cm}^2$, and the total resistance was $0.15\ \Omega\ \text{cm}^2$. The results suggest that very low pressure plasma spraying is a promising approach for the manufacturing of high-performance MS-SOFCs.

Keywords electrolyte · scandia-stabilized zirconia · solid oxide fuel cells · triple phase boundaries · very low pressure plasma spraying

Introduction

With the widespread use of fossil fuels and intensification of the greenhouse effect, effective and clean fuel utilization technology has become a key societal issue. Solid oxide fuel cells (SOFCs) are electrochemical devices that can directly and efficiently transform chemical energy to electronic energy. As a result, SOFCs technology has seen a rapid growth in recent years. However, the high manufacturing cost and low start-up speed have limited the commercialization of SOFCs. In recent years, one of the major research focuses has been to reduce the operation temperature from high temperature (800-1000 °C) to intermediate temperature (600-800 °C) (Ref [1]).

As the ionic conductivity of the electrolytes decreases exponentially with temperature, it is essential to develop the electrolyte materials with high conductivity. ScSZ is an attractive zirconia-based electrolyte with fluorite structure, which is of higher oxygen ion conductivity in the temperature range of 600-800 °C. In more detail, the ion conductivity of ScSZ electrolyte at 780 °C is $0.14\ \text{S cm}^{-1}$, which is comparable with the conductivity of yttria-stabilized zirconia electrolyte (YSZ) at 1000 °C (Ref [2]). SOFCs with ScSZ electrolytes exhibit superb performance (Ref [3], [4]), indicating that ScSZ is one of the most promising electrolyte materials at intermediate temperature. On the other hand, when SOFCs operate below 750 °C, it is

✉ Cheng-xin Li
licx@mail.xjtu.edu.cn

Yue-peng Wang
wangyuepeng@stu.xjtu.edu.cn

1 State Key Laboratory for Mechanical Behavior of Materials, School of Materials Science and Engineering, Xi'an Jiaotong University, Xi'an 710049, Shaanxi Province, People's Republic of China

possible to use the porous metal substrate as the support of cell. Actually, there has been a tendency to use the metal support in place of the anode support in recent years (Ref 5). The advantages of metal-supported (MS) SOFCs include low manufacturing costs, good resistance for mechanical disturbance and the ability to start up quickly. A number of reports have shown that MS-SOFCs exhibit excellent performance and long-term stability at intermediate temperature (Ref 6, 7).

However, there are only a few reports on metal-supported SOFCs with ScSZ electrolyte because of the challenges in cell preparation (Ref 4, 8). As specified earlier, electrolyte is the most important component in SOFCs. The fabrication process of electrolyte can determine the membrane structure and ultimately affect the performance of the entire cells. The fabrication of ceramic-supported SOFCs generally involves screen printing, slurry coating and tape casting. However, all of these wet chemical methods require subsequent sintering treatment to obtain strength. Electrolyte materials generally undergo the highest densification sintering temperature to acquire gas tightness, which involves a temperature of at least 1200 °C for co-sintering. For MS-SOFCs, the sintering of cells must be under reduced atmosphere to prevent the oxidization of metal support. Actually, MS-SOFCs face several issues under high-temperature sintering. While investigating high-temperature interfacial diffusion between Crofer22 APU alloy and nickel, Brandner et al. (Ref 9) concluded that chromium could diffuse to nickel coating within 70 μm after sintering 3 h at 1100 °C. Chromium poisoning can be a serious problem for MS-SOFCs. In addition, the sintering and coarsening of nickel in the anode were extremely serious under high-temperature reducing atmosphere. Therefore, the density of three-phase boundary (TPB) was significantly reduced (Ref 10).

As high-temperature sintering process limits the promotion of MS-SOFCs, atmosphere plasma spraying (APS) can be an attractive method to directly fabricate the coatings without sintering and shrinkage. The plasma spray process presents several advantages in the fabrication of MS-SOFCs, such as cost-effectiveness and easier to automate production. However, in the APS coatings, there are a large number of voids, non-bonded interfaces and vertical cracks, in which oxidant and fuel gas might leak and diffuse (Ref 11). Hence, without additional processing, electrolyte prepared by the APS method cannot be directly used in the solid oxide fuel cells due to the insufficient gas tightness and low conductivity. Li et al. (Ref 12) used the nitrate solution to infiltrate as-sprayed coatings and notably improved the gas tightness of YSZ electrolyte. In the report of Yao et al. (Ref 13), ion conductivity and gas tightness of the electrolyte improved by increasing the preheating temperature of the substrate. Zhang et al. (Ref 14) also

proved that the porosity of YSZ electrolyte decreased visibly with further increase in deposition temperature to 600 °C. Most of the columnar grains in the coatings could grow to a length over 10 μm. However, metal supports are super-sensitive to heat during the process. Hence, it is not suitable to heat the substrate to a temperature of more than 600 °C. Therefore, how to directly prepare dense electrolytes by thermal spraying remains a challenge for MS-SOFCs.

Very low pressure plasma spraying (VLPPS, usually operating at the chamber pressure of 100-1000 Pa) is a novel chamber plasma technology (Ref 15)for the preparation of electrolytes. When the pressure of the chamber decreases to 100 Pa, the plasma jet can become faster and larger (Ref 16). The plasma stream of a LPPS (low-pressure plasma spraying, usually operating at less than 50,000 Pa) system can be up to 2 m in length and 0.3 m in diameter. Using higher electrical input power, powders can melt completely in the long spraying distance and perhaps deposit from the vapor phase. The coatings deposited by LPPS can be typically featherlike columnar structure or porous structure due to the difference in parameters (Ref 17). The conductivity of grains with vertical orientation can be significantly improved in the vertical direction due to the decrease in the grain boundary density. However, loose columnar structure would lead to a reduction in the gas tightness. Hence, pure LPPS columnar structure coating cannot be directly used in the SOFCs electrolyte. When output power of plasma arc is decreased to 60 kW, the coating is primarily deposited in the liquid phase. Due to the longer deposition distance of samples, powders in flight can be well heated and accelerated. Therefore, the bond rate of the coatings would be much improved. A denser structure can be formed, and advantages of both the methods can be combined.

The purpose of this study is to fabricate dense electrolyte which can be directly used in SOFCs by VLPPS technology. In this study, the development of the microstructure of ScSZ coatings was investigated. The spraying distance was set to 150, 250 and 350 mm. The fractured cross-morphology and polished cross-microstructure were used to characterize the coatings bonding state. In addition, button MS-SOFCs with plasma-sprayed electrolyte were tested, obtaining high operating voltage and excellent power density.

Experimental

Materials and Methods

As is well-known, ScSZ has highest ionic conductivity in the zirconia-based electrolyte. ScSZ (ZrO_2-10%Sc_2O_3,

Fujimi, Japan) was used as the electrolyte material in this study. Typical morphology of ScSZ is shown in Fig. 1(a). ScSZ powder showed an essential lognormal large distribution with characteristic particle sizes of 9 μm (d_{10}), 18 μm (d_{50}) and 31 μm (d_{90}) (Fig. 1b). Commercial porous 430L stainless steel pellets (Gaoqian, China) were used for the cell support. Commercial $La_{0.6}Sr_{0.4}Co_{0.2}Fe_{0.8}O_{3-\delta}$ powders (Metco 6830A, Sulzer Metco, Westbury, USA) and agglomerated NiO/ScSZ (Tianyao, China) were used in this experiment to deposit cathode and anode, respectively.

Electrolyte coatings were deposited by a plasma spraying system (MF-P 1000APS/VPS, 80 kW, GTV, Germany) in a customized vacuum chamber (1-10^5 Pa, Dewei, China). To investigate the deposition behavior of coatings, a plasma torch of 60 kW output power was applied in this experiment at spraying distances of 150, 250 and 350 mm. The pressure of the chamber was set to 100 Pa. The microstructure was characterized using field emission scanning electron microscope (MIRA3 LMH, TESCAN, Czech Republic). The phase of the electrolyte coatings and powders was determined via x-ray diffraction (XRD-6000, Shimadzu, Japan). Thirty different SEM micrographs at 6000× magnification were considered for the porosity measurement via image analysis using the Image J software. The detailed steps can be found in the description on the official website of the software (Ref 18). A 3D confocal laser microscope was employed to measure the surface roughness and superficial area of the electrolyte coating. For the whole cells testing, anode and cathode were deposited by the APS method. The detailed preparation parameters of the anode and cathode can be found in our previous works (Ref 19, 20). In the electrochemical performance testing, Ag pastes were attached to the electrodes as the current collectors using the four terminals method.

As fuel, 95% H_2-5% H_2O for a total flow of 25 sccm was employed. Current voltage characteristics were recorded at different temperatures. A frequency response analyzer (Solartron 1260) and electrochemical interface analyzer (Solartron 1287) were used to measure the impedance data at open-circuit voltage. The amplitude was 10 mV in the temperature range from 600 to 750 °C. The frequency range was over 0.01 Hz to 0.1 MHz.

Results

Microstructure of the Sprayed ScSZ Coatings

As is shown in Fig. 2, original ScSZ powder contains zirconia in the tetragonal phase. However, after spraying, when material melting and solidification occurs, it was completely transformed into well-crystallized pure cubic zirconia phase with high electrical conductivity.

Figure 3(a), (b), (c), (d), (e), and (f) shows the typical fractured morphology of electrolyte coatings. Continuous columnar crystals clearly occured across the interlayer interface for all spraying distances. Generally, the thickness of the splat is about 1 μm under VLPPS condition, while in APS the thickness of the splat is much higher (Ref 14). However, the length of columnar crystals can be more than 10 μm, which is several times the thickness of splats. In addition, the density of unbonded interface decreases significantly as compared with typical APS coatings. The morphology of fractured cross section did not show clear differences for different spraying distances. This could be due to the good distance tolerance of the long plasma jet. Figure 4 exhibits the variation of deposition temperature during the plasma torch movement at the spraying distance of 250 mm, using an infrared radiation thermometer. The
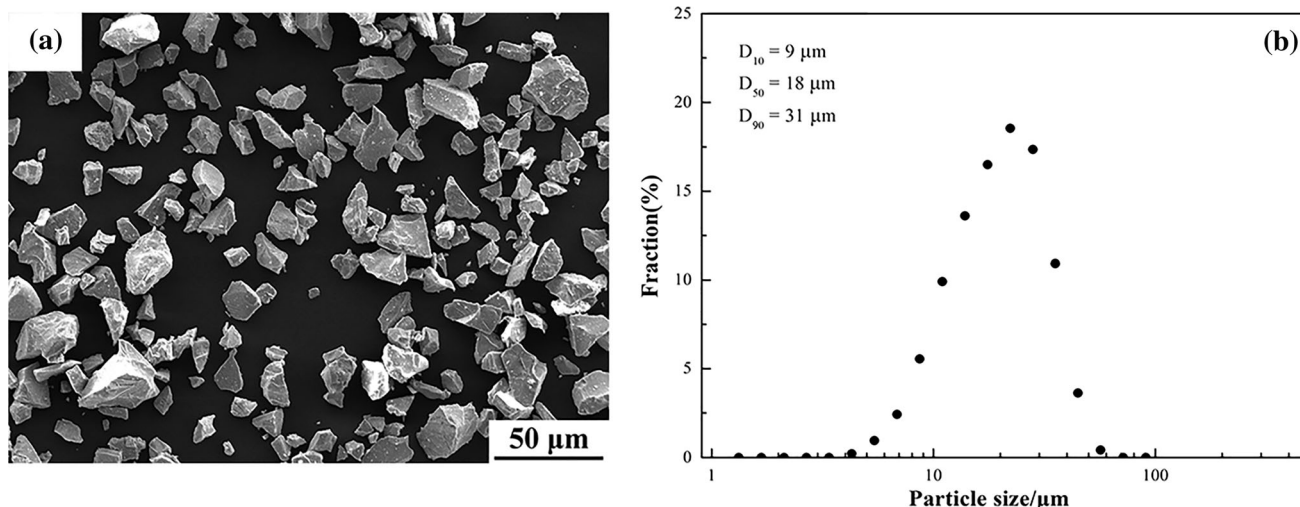

Fig. 1 Characteristic of original ScSZ powder (a) morphology and (b) particle size distribution

torch scanning speed was 0.8 m/s and scanning interval was 5 mm. In situ deposition temperature of coatings fluctuated with the movement of the plasma jet. Nevertheless, the deposition temperature generally did not exceed 350 °C. The interface temperature would be slightly lower at the distance of 350 mm and little higher at 150 mm due to the plasma jet energy decreasing with the increase in distance from outlet. However, this temperature is still much lower than the critical deposition temperature (600 °C) for the zirconia-based material (Ref 13). The higher temperature and velocity of particles can also affect the interlayer bonding rate. The extra internal energy and kinetic energy of the particles in low-pressure plasma

spraying could also provide an additional energy to overcome the energy barrier for forming effective bonding. In addition, we believe that with the increase in gas molecular free path in vacuum, the inner aperture of the ceramic coating is much smaller than the free path of the gas molecules. The gas-phase heat transfer can be neglected, and the surface convection heat transfer of the droplets is also limited during solidification. Otherwise, chemical modification of the surface also changes when the pressure is reduced. Fukumoto et al. (Ref 21) considered the effect of desorption of adsorbates on the particles flattening in the low-pressure plasma spraying process. The substrate temperature was maintained at room temperature. The transition from splash splat to disk-shaped one occurred by the reduction in surrounding pressure (Ref 22). The deposition under vacuum is quite different from atmosphere. The mechanism of this phenomenon can be discussed in the future work.

In order to understand the microstructure of ScSZ coatings, the polished cross section of the coatings was also characterized. Figure 5 reveals that the coatings were very dense, wherein no penetrating cracks occurred. The unbonded interface and vertical cracks were rare, and the number of longitudinal cracks was decreased. Although there were still some spherical pores in the coatings, the gas tightness of the coatings was significantly improved. The microstructure of the coatings did not change visibly for different spraying distances. Because of the longer deposition distance of low-pressure plasma spray, VLPPS can have a better deposition distance tolerance while the spraying distance for APS is usually about 100 mm. In the
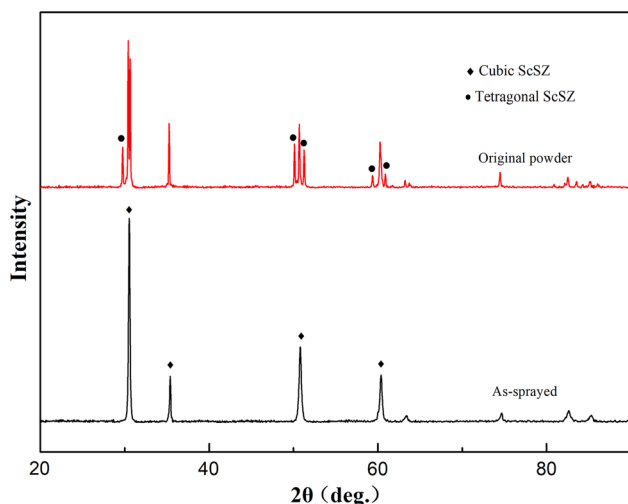

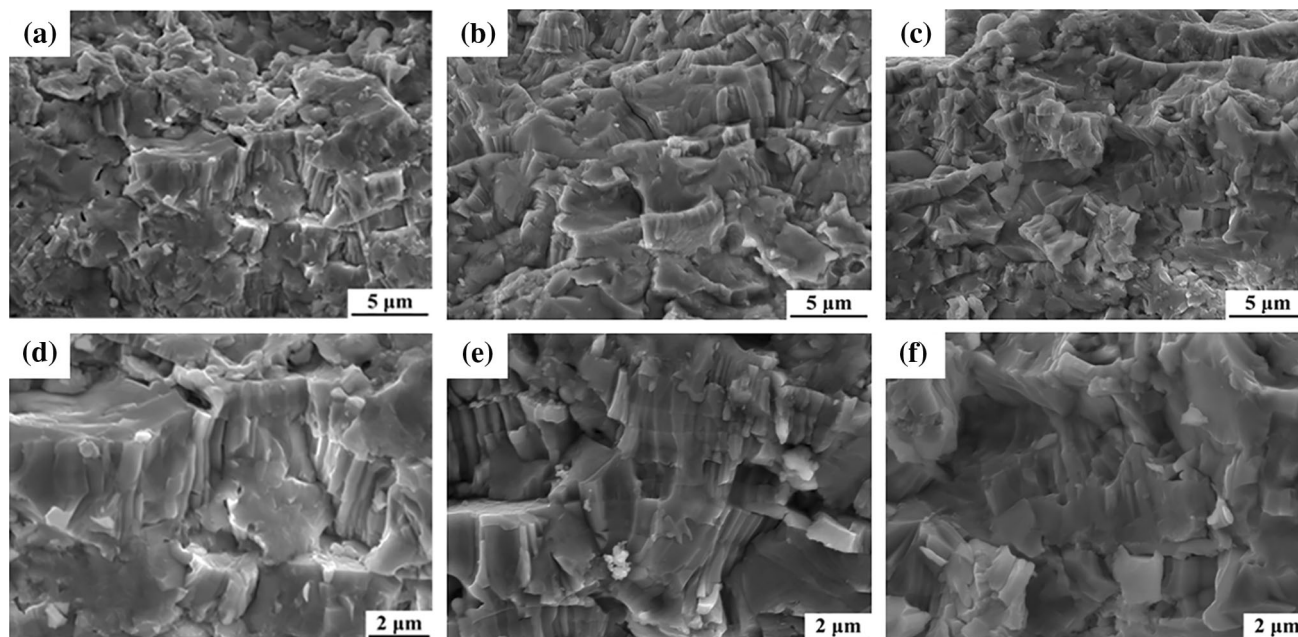Fig. 2 XRD pattern of ScSZ coatings and powders

Fig. 3 Fractured morphology of electrolyte at different spray distances: (a) (d) SD = 150 mm, (b) (e) SD = 250 mm and (c) (f) SD = 350 mm

long range of spraying distance, it can provide better structure uniformity for special structure SOFCs, such as corrugated cell and other cases. To quantify the compactness of the coatings, the porosity was calculated via image analysis method. As shown in Fig. 6, the apparent porosity of ScSZ coatings ranged from $4.75\% \pm 0.31\%$ to $6.83\% \pm 0.53\%$ due to the increase in interlayer bonding rate. The porosity was much lower than those of coatings by APS and LPPS (Ref 23). It is desirable that the conductivity and gas tightness of electrolyte coating are further improved.

Figure 7 shows the surface morphology of coatings deposited at different spraying distances. On the surface of the electrolyte, there were numerous bulges, which may be formed due to splash and random deposition of the liquid droplets. As shown in Fig. 7(b) and (e), the shape of the bulges became approximately spherical and the number of the bulges increased significantly at 250 mm compared with the other deposition distances. However, no visible

microcracks appeared on the surface of ceramic coatings. Generally, in the APS coatings, several microcracks would be found on the surface, which is because of quenching stress due to the large thermal gradient during rapid solidification. This can be an evidence for the decrease in surface convection heat transfer during the droplets solidification, which is discussed above.

Ionic Conductivity of ScSZ Coatings

As shown in Fig. 6, the coating with a spraying distance of 250 mm had the lowest porosity. To measure the conductivity of the coating, a ScSZ coating was firstly deposited on a nickel oxide support and then separated with the hydrochloric acid. A 100 ± 11-μm-thick freestanding coating was characterized by the AC impedance spectrum method. As shown in Fig. 8(a) and (b), the ionic conductivity of the coating at the spraying distance of 250 mm was 0.068 S cm^{-1} at the temperature of 750 °C, which is almost 68% of the conductivity of the bulk. The value is significantly higher than the conductivity of APS scandia-stabilized zirconia coatings reported by Li et al. (Ref 24).
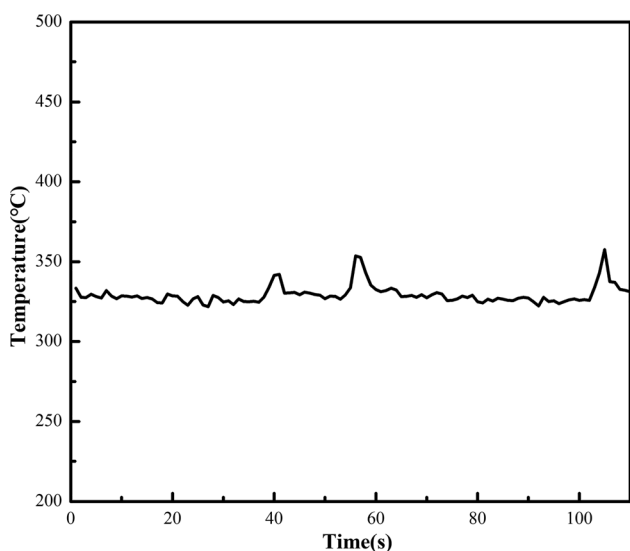
Fig. 4 Temperature fluctuation of substrate with time (torch scanning speed at 0.8 m/s)
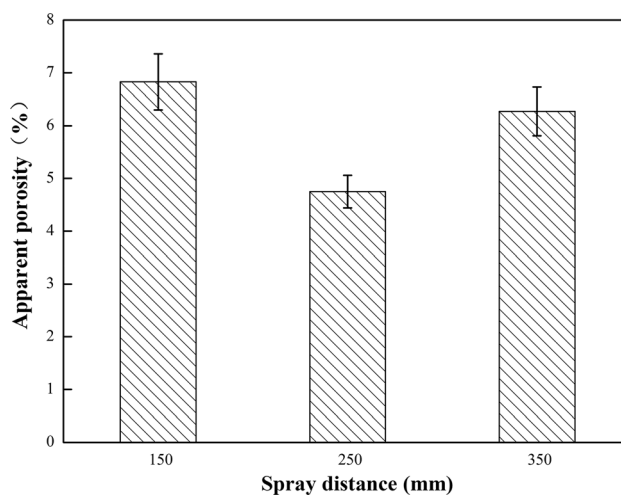
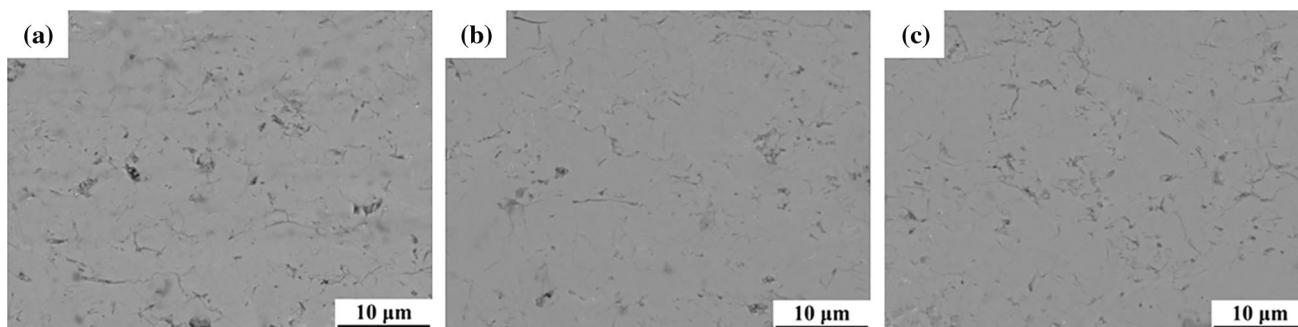Fig. 6 Porosity of coatings at different spraying distances

Fig. 5 Polished cross-sectional structure of coatings deposited at the spray distance: (a) 150 mm, (b) 250 mm and (c) 350 mm
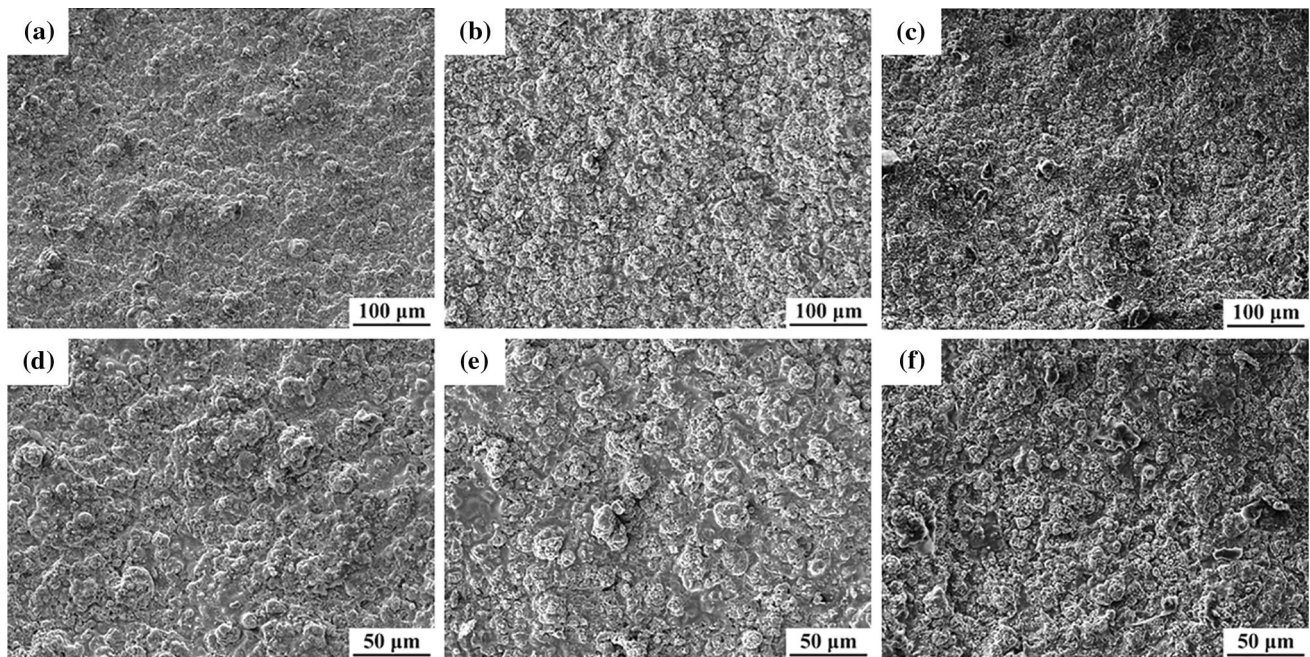
Fig. 7 Surface morphology of electrolyte at different spray distances under SEM: (a) (d) SD = 150 mm, (b) (e) SD = 250 mm and (c) (f) SD = 350 mm

The activation energy (E_a) for the oxide ion conductivity was 0.99 eV, as obtained from the Arrhenius plots (Fig. 8c), which is consistent with the value of bulk reported by Omar (Ref 25). Usually, the conductivity of the ScSZ deposit depends on the microstructure of the ceramics. As shown in Fig. 3(e), the remarkable increase in conductivity can be attributed to the continuous growth of columnar crystals across the splat interfaces. The lamellar structure and non-bonded interfaces regions with very low conductivity would cut off the ion transport pathways. With the decease in unbonded interfaces and cracks, oxygen ion could transport through the electrolyte deposits in a direction perpendicular to the lamellae.

Cell Performance

A whole cell with the structure of 430L∥NiO/ScSZ∥ScSZ∥LSCF was used to examine the output performance. The polished microstructure is shown in Fig. 9. The anode and cathode coatings of about 25 μm were fabricated by the APS process. The thickness of ScSZ electrolyte deposited at 250 mm was about 50 μm, which both ensured the gas tightness and reduced the ohmic loss of electrolyte. The output performances of the cell with ScSZ coating are shown in Fig. 10(a). The open-circuit voltage (OCV) of cell could reach 1.07 V at 750 °C, which is close to the theoretical voltage. The high OCV indicates that the gas tightness of the electrolyte was sufficient for SOFCs applications. The peak output power density

reached 1112 mW cm^{-2} at 750 °C. When the operating temperature was decreased to 700, 650, 600 and 550 °C, the maximum output power density could be 754, 469, 282 and 146 mW cm^{-2}, respectively. Figure 10(b) shows the Nyquist plots for whole cell under OCV condition. The ohmic resistance of whole cell was 0.1 Ω cm^2, and the total resistance of whole cell was 0.15 Ω cm^2 at 750 °C. These results show that the electrolyte coatings with high performance could be prepared by very low pressure plasma spraying for metal-supported solid oxide fuel cells.

Surface Morphology and Triple Phase Boundary

The high output performance can be attributed to the high ionic conductivity and high reactive area of interface, due to the decrease in the ohmic loss and the polarization loss of the cell. The spherical bulges on the electrolyte surface can increase the triple phase boundary (TPB) density for the reaction of oxygen reduction. The high TPB density (or length) could determine faster kinetics of the charge transfer reaction and enhance the cell performance (Ref 26, 27). In order to clarify the lower polarization resistance of the cells, a 3D confocal laser microscope was applied to analyze the surface morphology of the electrolyte at different spraying distances. As shown in Fig. 7, on the surface of the electrolyte there were numerous spherical bulges, which may be formed by the spatter or heterogeneous deposition of the liquid droplets. Notably, the electrolyte surface is the interface of the cathode and
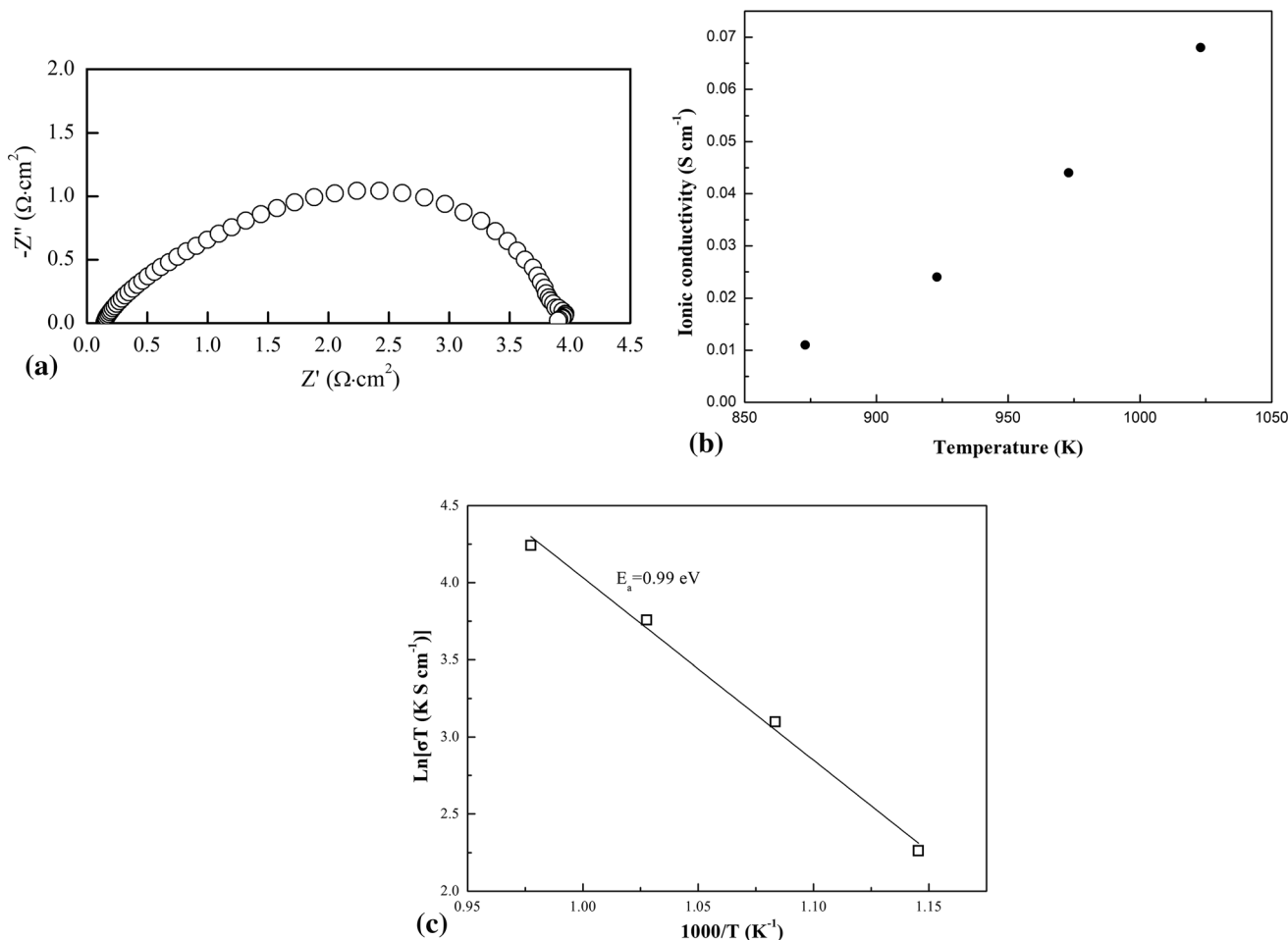
Fig. 8 Characterization of ScSZ coatings: (a) AC impedance spectrum result of the coating at the spraying distance of 250 mm at 750 °C, (b) influence of temperature on the electrical conductivity of the plasma-sprayed ScSZ coatings and (c) Arrhenius plots for the total ionic conductivity
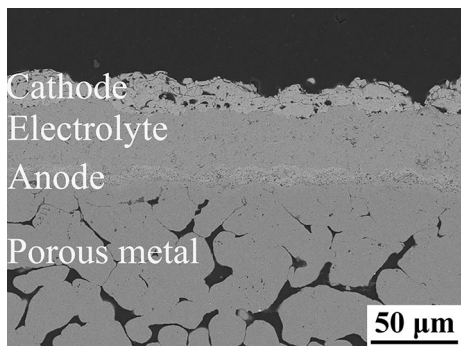

Fig. 9 Polished cross-sectional microstructure of the cell with VLPPS electrolyte

electrolyte. The high active area of the surface would significantly increase the length of TPB and enhance the performance of the cells. Herein, we define the ratio of surface area of electrolyte to its projected area to quantitatively measure the length of the TPB. As shown in Fig. 11, the large number of bulges on the surface led to a large active area of the electrolytes. The ratio of surface area to projected area could reach 6.53 ± 0.16 to 8.30 ± 0.37 measured in different conditions. This phenomenon may explain the high performance of SOFCs.

Conclusions

Dense electrolyte coatings with trans-granular structure were acquired via VLPPS technology at a relatively low deposition temperature (< 350 °C). The apparent porosity of ScSZ coating was 4.75-6.83% using image analysis method. The ionic conductivity of the sprayed coatings at 250 mm spraying distance could reach 0.068 S cm^{-1} at 750 °C, which is $\sim 68\%$ of the conductivity of bulk. Testing cells based on very low pressure plasma-sprayed ScSZ electrolyte showed a maximum output power density of 1111.6 mW cm^{-2} and an OCV of 1.07 V at 750 °C. The ohmic resistance of the whole cell was 0.1 Ω cm^2 and the total resistance of whole cell was 0.15 Ω cm^2, suggesting
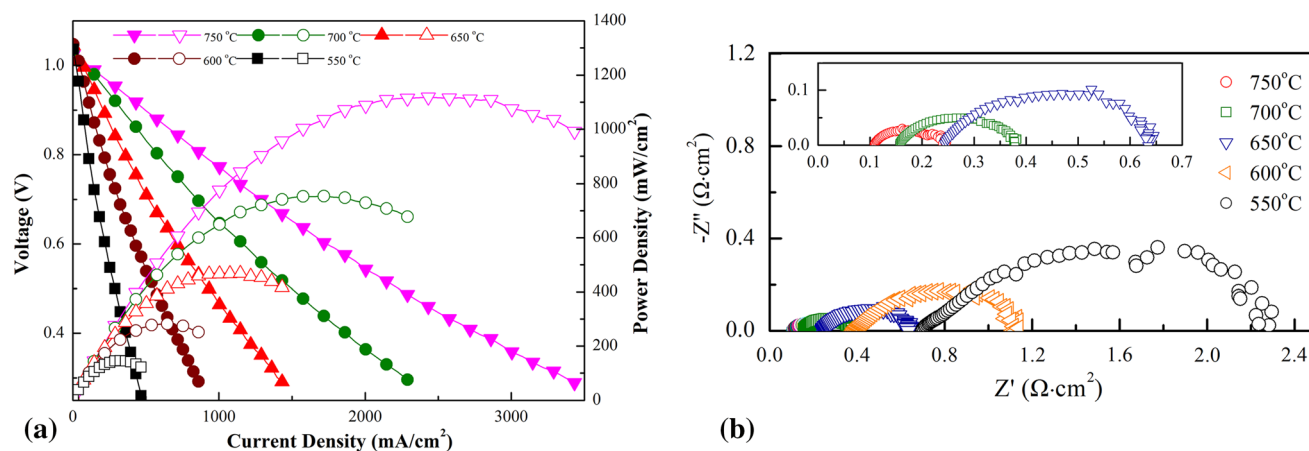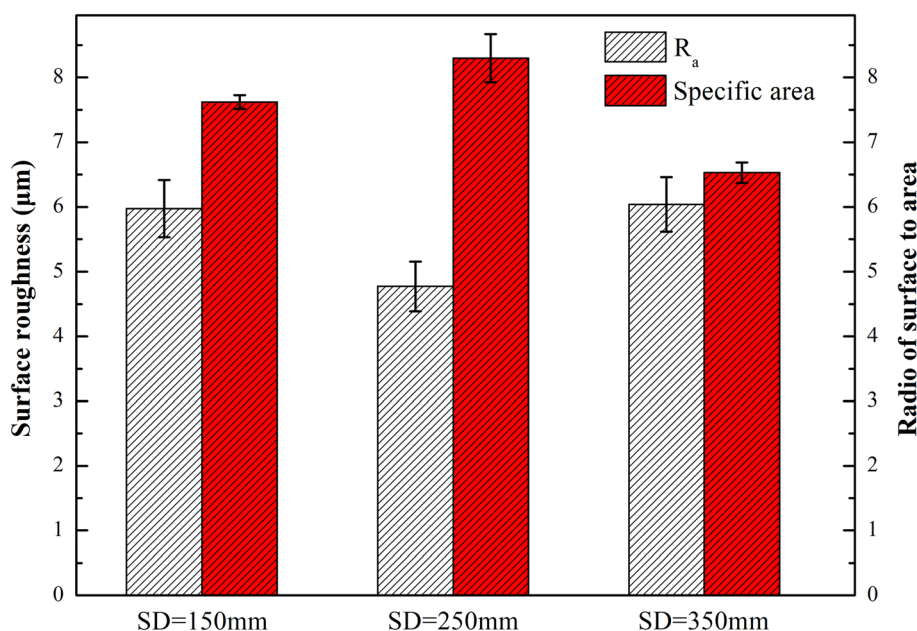
Fig. 10 Electrochemical performance of the cell: (a) output power performance at different deposition temperatures and (b) Nyquist plots

Fig. 11 Surface roughness and specific surface area for deposited distance obtained via 3D confocal laser microscope

that very low pressure plasma spraying is a promising approach for the manufacturing of high-performance MS-SOFCs. When using a 3D confocal laser microscope to characterize the top surface morphology of the electrolyte, the ratio of surface area to projected area of ScSZ coatings could reach 6.53-8.30, which may be related to the high performance of SOFCs.

References

1. A. Sinha, D. Miller, and J.T.S. Irvine, Development of Novel Titanium Oxycarbide Anode material for Intermediate Temperature SOFC (IT-SOFC), *J. Mater. Chem. A*, 2016, https://doi.org/10.1039/C6TA03404G

2. S. Omar, A. Belda, A. Escardino, and N. Bonanos, Ionic Conductivity Ageing Investigation of 1Ce10ScSZ in Different Partial Pressures of Oxygen, *Solid State Ionics*, 2011, **184**(1), p 2-5

3. H. Gu, R. Ran, Z. Wei, and Z. Shao, Anode-Supported ScSZ-Electrolyte SOFC with Whole Cell Materials from Combined EDTA–Citrate Complexing Synthesis Process, *J. Power Sources*, 2007, **172**(2), p 704-712

4. H. Shi, R. Ran, and Z. Shao, Wet Powder Spraying Fabrication and Performance Optimization of IT-SOFCs with Thin-Film ScSZ Electrolyte, *Int. J. Hydrogen Energy*, 2012, **37**(1), p 1125-1132

5. M.C. Tucker, G.Y. Lau, C.P. Jacobson, L.C. Dejonghe, and S.J. Visco, Performance of Metal-Supported SOFCs with Infiltrated Electrodes, *J. Power Sources*, 2007, **171**(2), p 477-482

6. D. Soysal, J. Arnold, P. Szabo, R. Henne, and S.A. Ansar, Thermal Plasma Spraying Applied on Solid Oxide Fuel Cells, *J. Therm. Spray Technol.*, 2013, **22**(5), p 588-598

7. M.C. Tucker, G.Y. Lau, C.P. Jacobson, L.C. Dejonghe, and S.J. Visco, Stability and Robustness of Metal-Supported SOFCs, *J. Power Sources*, 2008, **175**(1), p 447-451

8. S.-L. Zhang, C.-X. Li, C.-J. Li, G.-J. Yang, and M. Liu, Application of High Velocity Oxygen Fuel Flame (HVOF) Spraying to Fabrication of $La_{0.8}Sr_{0.2}Ga_{0.8}Mg_{0.2}O_3$ electrolyte for solid oxide fuel cells, *J. Power Sources*, 2016, **301**, p 62-71

9. M. Brandner, M. Bram, J. Froitzheim, H.P. Buchkremer, and D. Stöver, Electrically Conductive Diffusion barrier layers for Metal-Supported SOFC, *Solid State Ionics*, 2008, **179**(27), p 1501-1504

10. I. Villarreal, C.P. Jacobson, A. Leming, Y. Matus, S.J. Visco, and L.D. Jonghe, Metal-Supported Solid Oxide Fuel Cells, *Electrochem. Solid State Lett.*, 2003, **6**(9), p A178

11. C.J. Li, C.X. Li, Y.Z. Xing, M. Gao, and G.J. Yang, Influence of YSZ Electrolyte Thickness on the Characteristics of Plasma-Sprayed Cermet Supported Tubular SOFC, *Solid State Ionics Diffus. React.*, 2006, **177**(19–25), p 2065-2069

12. C.X. Li, C.J. Li, and G.J. Yang, Development of a Ni/Al_2O_3 Cermet-Supported Tubular Solid Oxide Fuel Cell Assembled with Different Functional Layers by Atmospheric Plasma-Spraying, *J. Therm. Spray Technol.*, 2009, **18**(1), p 83-89

13. S.W. Yao, C.J. Li, J.J. Tian, G.J. Yang, and C.X. Li, Conditions and Mechanisms for the Bonding of a Molten Ceramic Droplet to a Substrate After High-Speed Impact, *Acta Mater.*, 2016, **119**, p 9-25

14. S.-L. Zhang, C.-X. Li, and C.-J. Li, Plasma-Sprayed Y_2O_3-Stabilized ZrO_2 Electrolyte with Improved Interlamellar Bonding for Direct Application to Solid Oxide Fuel Cells, *J. Fuel Cell Sci. Technol.*, 2014, **11**(3), p 031005

15. J.L. Dorier, M. Gindrat, C. Hollenstein, M. Loch, A. Refke, A. Salito, G. Barbezat, Plasma jet properties in a new spraying process at low pressure for large area thin film deposition, *Lrp* (2001)

16. K.V. Niessen, M. Gindrat, and A. Refke, Vapor Phase Deposition Using Plasma Spray-PVD^{TM}, *J. Therm. Spray Technol.*, 2010, **19**(1–2), p 502-509

17. A. Hospach, G. Mauer, R. Vaßen, and D. Stöver, Columnar-Structured Thermal Barrier Coatings (TBCs) by Thin Film Low-Pressure Plasma Spraying (LPPS-TF), *J. Therm. Spray Technol.*, 2011, **20**(1–2), p 116-120

18. ImageJ, http://imagej.en.softonic.com/. Accessed 12 May 2018

19. S.-L. Zhang, C.-X. Li, C.-J. Li, G.-J. Yang, and Z.-H. Han, Scandia-Stabilized Zirconia Electrolyte with Improved Interlamellar Bonding by High-Velocity Plasma Spraying for High Performance Solid Oxide Fuel Cells, *J. Power Sources*, 2013, **232**, p 123-131

20. S.-L. Zhang, T. Liu, C.-J. Li, S.-W. Yao, C.-X. Li, G.-J. Yang, and M. Liu, Atmospheric Plasma-Sprayed $La_{0.8}Sr_{0.2}Ga_{0.8}Mg_{0.2}O_3$ Electrolyte Membranes for Intermediate-Temperature Solid Oxide Fuel Cells, *J. Mater. Chem. A*, 2015, **3**(14), p 7535-7553

21. M. Fukumoto, Y. Tanaka, and E. Nishioka, Flattening Problem of Thermal Sprayed Particles, *Mater. Sci. Forum*, 2004, **449–452**(2), p 1309-1312

22. K. Yang, M. Liu, K. Zhou, and C. Deng, Recent Developments in the Research of Splat Formation Process in Thermal Spraying, *J. Mater.*, 2012, **2013**(2), p 1-14

23. C. Zhang, H.L. Liao, W.Y. Li, G. Zhang, C. Coddet, C. Zhang, C.J. Li, C.X. Li, and X.J. Ning, Characterization of YSZ Solid Oxide Fuel Cells Electrolyte Deposited by Atmospheric Plasma Spraying and Low Pressure Plasma Spraying, *J. Therm. Spray Technol.*, 2006, **15**(4), p 598-603

24. C.X. Li, C.J. Li, H.G. Long, Y.Z. Xing, X.J. Ning, C. Zhang, H.L. Liao, and C. Coddet, Characterization of Atmospheric Plasma-Sprayed Sc_2O_3–ZrO_2 Electrolyte Coating, *Solid State Ionics*, 2006, **177**(19), p 2149-2153

25. S. Omar, W.B. Najib, W. Chen, N. Bonanos, and B. Dunn, Electrical Conductivity of 10 mol% Sc_2O_3–1 mol% M_2O_3–ZrO_2 Ceramics, *J. Am. Ceram. Soc.*, 2012, **95**(6), p 1965-1972

26. M.S. Khan, W. Wahyudi, S.B. Lee, R.H. Song, J.W. Lee, T.H. Lim, and S.J. Park, Effect of Various Sintering Inhibitors on the Long Term Performance of Ni-YSZ Anodes Used for SOFCs, *Int. J. Hydrogen Energy*, 2015, **40**(35), p 11968-11975

27. T. Horita, K. Yamaji, N. Sakai, Y. Xiong, T. Kato, H. Yokokawa, and T. Kawada, Imaging of Oxygen Transport at SOFC Cathode/Electrolyte Interfaces by a Novel Technique, *J. Power Sources*, 2002, **106**(1), p 224-230